HHS Public Access

Author manuscript

Chem Biol Interact. Author manuscript; available in PMC 2019 July 15.

Published in final edited form as:

Chem Biol Interact. 2018 December 25; 296: 45–56. doi:10.1016/j.cbi.2018.09.001.

The roles of breast cancer resistance protein (BCRP/ABCG2) and multidrug resistance-associated proteins (MRPs/ABCCs) in the excretion of cycloicaritin-3-*O*-glucoronide in UGT1A1-overexpressing HeLa cells

Shishi Li[a,1], **Jinjin Xu**[a,1], **Zhihong Yao**[a,b,*], **Liufang Hu**[a], **Zifei Qin**[a,c,**], **Hao Gao**[a,b], **Kristopher W. Krausz**[d], **Frank J. Gonzalez**[d], and **Xinsheng Yao**[a,b]

[a]College of Pharmacy, Jinan University, Guangzhou, 510632, PR China

[b]Guangdong Provincial Key Laboratory of Pharmacodynamic Constituents of TCM and New Drugs Research, College of Pharmacy, Jinan University, Guangzhou, 510632, PR China

[c]Department of Pharmacy, The First Affiliated Hospital of Zhengzhou University, Zhengzhou, 450052, PR China

[d]Laboratory of Metabolism, Center for Cancer Research, National Cancer Institute, National Institutes of Health, Bethesda, MD, 20892, USA

Abstract

Cycloicaritin is a bioactive natural phenolic compound from *Epimedium* species. However, the glucuronidation and excretion which would influence oral bioavailability and pharmacokinetics of cycloicaritin still remain unknown. Here we aimed to establish UGT1A1 stably transfected HeLa cells, and to determine the contributions of BCRP and MRPs transporters to excretion of cycloicaritin-3-*O*-glucuronide. First, β-estradiol was used to validate the expression of active UGT1A1 protein in engineered HeLa1A1 cells. Furthermore, Ko143 (5 and 20 μM) led to a significant decrease (42.4%–63.8%, $p < 0.01$) in CICT-3-G excretion and obvious accumulation (19.7%–54.2%, $p < 0.05$) of intracellular CICT-3-G, while MK571 (5 and 20 μM) caused a significant reduction (46.8%–64.8%, $p < 0.05$) in the excretion and obvious elevation (50.7%–85.2%, $p < 0.01$) of intracellular level of CICT-3-G. Furthermore, BCRP knocked-down brought marked reduction in excretion rates of CICT-3-G (26.0%–42.2%, $p < 0.01$), whereas MRP1 and MRP4-mediated silencing led to significant decrease in the excretion of CICT-3-G (23.8%–35.4%, $p < 0.05$ for MRP1 and 11.9%–16.0%, $p < 0.05$ for MRP4). By contrast, neither CICT-3-G excretion nor CICT-3-G accumulation altered in MRP3 knocked-down cells as compared to

[*]Corresponding author. College of Pharmacy, Jinan University, Guangzhou, 510632, PR China. yaozhihong_jnu@163.com, yaozhihong.jnu@gmail.com (Z. Yao). [**]Corresponding author. College of Pharmacy, Jinan University, Guangzhou, 510632, PR China. qzf1989@163.com (Z. Qin).

[1]These authors contributed equally to this work.

Conflicts of interest

All the authors report no declarations of interest.

Transparency document

Transparency document related to this article can be found online at https://doi.org/10.1016/j.cbi.2018.09.001.

Appendix A. Supplementary data

Supplementary data to this article can be found online at https://doi.org/10.1016/j.cbi.2018.09.001.

scramble cells. Taken together, BCRP, MRP1 and MRP4 were identified as the most important contributors for CICT-3-G excretion. Meanwhile, the UGT1A1 modified HeLa cells were a simple and practical tool to study UGT1A1-mediated glucuronidation and to characterize BCRP and MRPs-mediated glucuronide transport at a cellular level.

Keywords

Cycloicaritin; UGT1A1; Glucuronidation; HeLa cells; Efflux transporters

1. Introduction

Glucuronidation mediated by human UDP-glucuronosyltransferases (UGTs) is a principal phase II reaction for the clearance of exogenous drugs (antipsychotics, tricyclic antidepressants, antineoplastic drugs, etc) [1] and endogenous substances (steroids, bilirubin, hormones, etc) [2]. It is well-accepted that glucuronidation is responsible for about 35% drugs metabolized by phase II enzymes [3]. Besides, 15% of the 200 most prescribed drugs in the United States of America (USA) are cleared directly *via* glucuronidation pathway [4]. In addition, as one of the most important UGT enzyme, human UGT1A1 catalyzed approximately 15% of marketed drugs, mainly including irinotecan, SN-38, ethynylestradiol, cyproheptadine and morphine [1]. On the other hand, UGT1A1 plays an important role in maintaining stable balance of bilirubin, bile acids and estrogen levels in human [5]. The abnormality or deficiency of UGT1A1 *in vivo* is highly associated with some diseases (Gilbert syndrome, Crigler-Najjar syndrome, Hyperbilirubinemia) [6], efficacy and toxicity of drugs, and precisely therapeutic personality. Hence, it is of great clinical significance to study the metabolism by UGT1A1 enzyme.

Of note, the excretion of glucuronides from intracellular to extracellular requires two processes, glucuronides formation and excretion [7]. Once the glucuronides are formed by UGTs, the soluble metabolites are transported out the cell, in many instances through high affinity efflux transporters, and become sequestered in the water compartments of the tissue that eventually lead to elimination. Drug transporters including P-glycoprotein (P-gp), breast cancer resistance protein (BCRP), and multidrug resistance-associated proteins (MRPs), are characterized to be distributed in the apical cellular membranes of the liver, intestine, kidney and brain, preventing our body from exogenous toxicants [8]. Meanwhile, BCRP and MRPs are members of the C subfamily of ATP-binding cassette (ABC) transporters, which mediate active transport of their substrates across cell membranes using the energy of ATP binding and hydrolysis [9]. Besides, P-gp mostly transports cationic and neutral compounds, while BCRP and MRPs transport anions such as the glucuronides [10]. Meanwhile, the *in vivo* exposure of xenobiotics is driven by phase II metabolic enzymes and efflux transporters in $BCRP^{-/-}$ and $MRP^{-/-}$ mice, which indicated that murine BCRP and/or MRPs contribute significantly to the excretion of glucuronides [11-13]. Therefore, understanding the roles of BCRP and MRPs are important in glucuronide disposition and/or in determining the rate-limiting step (metabolism vs excretion) in cellular glucuronide production.

Cycloicaritin (CAS No. 38226-86-7), also called β-anhydroicaritin, was a natural effective flavone occurring in several *Epimedium* species (Berberidaceae family) [14]. It has already exhibited numerous biological activities, including anti-osteoporosis effects, anti-inflammatory effects, antimicrobial and PPAR-γ ligand binding activity, inhibiting P-gp efflux function and significantly down-regulated on the expression of P-gp preotein [15-18]. Meanwhile, cycloicaritin could serve as a leading agent for pharmacological control of metabolic diseases, since cycloicaritin improves diet-induced obesity and alleviates insulin resistance by suppressing sterol regulatory element-binding proteins (SREBPs) maturation which is dependent on LKB1/AMPK/mTOR pathway [15]. Moreover, anti-osteoporosis effects and bioavailability of cycloicaritin-suet oil-sodium deoxycholate self-assembled nanomicelles were significantly increased due to an increase in absorption by reducing the particle sizes of cycloicaritin [19]. The biological properties of flavones are well known to be severely limited by the compound's low bioavailability resulting from extensive metabolism and excretion [20-22]. However, the action mechanism and characteristics of the metabolism and excretion of cycloicaritin still remain unclear.

In this study, we found that cycloicaritin could be efficiently metabolized to cycloicaritin-3-*O*-glucuronide by UGT1A1. To better understand the UGT1A1-catalyzed glucuronidation and efflux transports-mediated excretion of cycloicaritin, UGT1A1 enzyme was stably transfected to HeLa cells to catalyze the glucuronidation of cycloicaritin. Furthermore, chemical inhibitors (Ko143, MK571, dipyridamole and leukotriene C4) and biological knock-down assays [short hairpin RNA (shRNA)-mediated silencing of a target transporter] were performed to investigate the roles of efflux transporters. The results would be valuable in achieving better prediction of cycloicaritin disposition, which could be the main factors affecting its bioavailability and biological activities. In addition, the findings could also add our general understanding of the action mechanisms of cycloicaritin *in vivo.* Moreover, this cell model provided a practical and feasible approach to evaluate the UGT-catalyzed glucuronidation and efflux transports-mediated excretion of clinical drugs and xenobiotics.

2. Materials and methods

2.1. Materials

Alamethicin, β-estradiol, dipyridamole (DIPY), D-saccharic-1, 4-lactone, magnesium chloride ($MgCl_2$), MK-571, Ko143, leukotriene C4 (LTC4) and uridine diphosphate glucuronic acid (UDPGA) were all obtained from Sigma-Aldrich (St Louis, MO). Apigenin, chrysin, cycloicaritin, genistein, and wushanicaritin with purity over 98% was purchased from Aladdin Reagents (Shanghai, China). Apigenin-7-*O*-glucuronide, chrysin-7-*O*-glucuronide, genistein-7-*O*-glucuronide, and β-estradiol-3-*O*-glucuronide was purchased from Toronto Research Chemicals (North York, ON, Canada). Wushanicaritin-3-*O*-glucuronide was prepared in our laboratory as described previously [23]. 293T cells, HeLa cells, pLVX-mCMV-ZsGreen-PGK-Puro vector [9371 base pairs (bp)] and pLVX-shRNA2-Neo vector (9070 bp) were all provided from BioWit Technologies (Shenzhen, China). The pGEM-T plasmid which carried the UGT1A1 cDNA clone was purchased from Sino Biological Inc. (Beijing, China), while recombinant human UGT1A1 was purchased from Corning Biosciences (New York, USA). The anti-BCRP, anti-GAPDH, anti-MRP1, anti-

MRP2, anti-MRP3, anti-MRP4 and anti-UGT1A1 antibodies were all obtained from OriGene Technologies (Rockville, MD). All other chemicals and reagents were the highest grade commercially available.

2.2. Establishment of UGT1A1-overexpressing HeLa cells

As published previously [23,24], the development of UGT1A1-overexpressing HeLa cells mainly underwent three steps. Firstly, the purified fragment of UGT1A1 cDNA (1602 bp) was obtained after the restriction of BamHI and MluI were introduced in pGEM-T-UGT1A1 plasmid. The cloned genes were sequenced within the vector construct and were found to be identical to the known genomic sequence (NM_000463.2). Secondly, based on the third-generation packaging system from BioWit technologies, lentiviral vectors were produced by transient transfection into 293T cells. Finally, HeLa cells were transfected by incubation with the lentivirus. The stably transfected HeLa cells were cryopreserved for future use. The multiplicity of infection (MOI) value was 10 in stable transfection of HeLa cells. The UGT1A1 modified HeLa cells are named HeLa1A1 cells.

2.3. Transient transfection of shRNA plasmids

The shRNA plasmids for efflux transports including BCRP, MRP1, MRP2 and MRP4 were constructed as described in previous studies [23,24]. Each pair of shRNA was ligated into the pLVX-ShRNA2-Neo plasmid. The shRNA fragments within the vector construct were sequenced using the primer U6—F (5′-TACGATACAAGGCTGTTAGA GAG-3′) by Invitrogen (Carlsbad, CA). Further, HeLa1A1 cells were transiently transfected with the corresponding shRNA plasmids. Briefly, the HeLa1A1 cells were cultured at a density of 2.0×10^5 cells/well in a 6-well plate. After 48 h, the control scramble, shRNA-BCRP, shRNA-MRP1, shRNA-MRP2 and shRNA-MRP4 plasmids (4 μg) were individually transfected into HeLa1A1 cells using the Polyfectine transfection reagent (Biowit Technologies, Shenzhen, China). The HeLa1A1 cells silencing BCRP, MRP1, MRP3 or MRP4 proteins could be ready for excretion experiments after transfection for 2 days. The established cells were named as HeLa1A1-BCRP-shRNA cells, HeLa1A1-MRP1-shRNA, HeLa1A1-MRP3-shRNA, and HeLa1A1-MRP4-shRNA cells, respectively.

2.4. Preparation of HeLa1A1 cell lysate

HeLa1A1 cells were collected in 50 mM Tris-HCl buffer (pH 7.4), following disrupting by sonication for 1 min. Protein concentration was determined by the Bio-Rad protein assay kit using bovine serum albumin as a standard.

2.5. Cycloicaritin-3-O-glucuronidation assay

Glucuronidation activities of cycloicaritin by recombinant UGT1A1 and HeLa1A1 cell lysate were measured as mentioned previously [23-26]. The mixture (200 μL) was incubated at 37 °C. After incubation for 2 h, the reaction was terminated using ice-cold acetonitrile (200 μL). The samples were mixed and centrifuged at 13800 g for 10 min. The supernatant was subjected to ultra-high-performance liquid chromatography (UHPLC) analysis.

2.6. Enzymes kinetic evaluation

A series of cycloicaritin (0.1–10 μM, final concentrations) were incubated with recombinant UGT1A1 and HeLa1A1 cell lysate to determine the rates of cycloicaritin-3-*O*-glucuronidation. The kinetic model Hill equation was fitted to the data of metabolic rates *versus* cycloicaritin concentrations and displayed in Equation (1). Appropriate model was also selected by visual inspection of the Eadie-Hofstee plot [27]. The parameters were as follows. V is the formation rate of product. V_{max} is the maximal velocity. S is the substrate. S_{50} is the substrate concentration resulting in 50% of V_{max} and n is the Hill coefficient. The maximal clearance (CL_{max}) was obtained using Equation (2). Model fitting and parameter estimation were performed by Graphpad Prism V5 software (SanDiego, CA).

$$V = \frac{V\max \times [S]^{n}}{S_{50}^{n} \times [S]^{n}} \quad (1)$$

$$V = \frac{V\max}{S_{50}} \times \frac{n-1}{n(n-1)^{1/n}} \quad (2)$$

2.7. Excretion assays

The excretion experiments of β-estradiol-3-*O*-glucuronide, wushanicaritin-3-*O*-glucuronide, apigenin-4′—*O*-glucuronide, chrysin-7-*O*-glucuronide, genistein-7-*O*-glucuronide, and CICT-3-*O*-G were performed as published previously [23,24]. Chemical inhibitors (Ko143, MK571, DIPY and LTC4) were co-incubated with Hank's buffered salt solution (HBSS) containing wushanicaritin (1 μM), apigenin (5 μM), chrysin (10 μM), genistein (5 μM), and cycloicaritin (8 μM) in HeLa1A1 cells to determine the roles of BCRP and MRPs, while four shRNAs transfected HeLa1A1 cells were only treated with HBSS containing cycloicaritin (8 μM) to investigate the detailed roles of BCRP, MRP1, MRP3 and MRP4 in the excretion of CICT-3-*O*-G, respectively. At 0.5, 1, 1.5 and 2h, incubation medium (200 μL) was withdrew and immediately replenished with equal volume of dosing solution. Equal volume of ice-cold acetonitrile was added and centrifuged at 13800 g for 10 min. The supernatant were tested by UHPLC or UHPLC-MS to determine the concentrations of corresponding glucuronides. At 2 h, the cells were collected and treated using sonication for 1 min to measure the amounts of intracellular corresponding glucuronides. Further, the intracellular concentration of corresponding glucuronides was estimated as the intracellular amount since the intracellular volume of the cells was assumed to be 4 mL/mg protein [28].

The excretion rate of intracellular corresponding glucuronides was calculated according to Equation (3). The apparent efflux clearance (CL_{app}) for corresponding glucuronides was derived by ER/C_i, where C_i is the intracellular concentration of corresponding glucuronides. The fraction metabolized value (f_{met}) reflected the extent of the glucuronidation in the cells and was calculated as Equation (4). Where V is the volume of the incubation medium; C is

the cumulative concentration of corresponding glucuronides; and t is the incubation time. Here, dC/dt describes the changes of the corresponding glucuronides levels with time.

$$\text{Excretion rate (ER)} = v\frac{dC}{dt} \quad (3)$$

$$f_{met} = \frac{\text{excreted glucuronide+intracellular glucuronide}}{\text{dosed aglycine}} \quad (4)$$

2.8. Quantification of cycloicaritin and cycloicaritin-3-O-glucuronide

Quantification of cycloicaritin and cycloicaritin-3-*O*-glucuronide was performed using an Acquity™ UHPLC I-Class system (Waters Corporation, Manchester, U.K.). Chromatographic separation was achieved on a BEH C18 column (2.1 mm × 50 mm, 1.7 μm, Waters, Ireland, Part NO. 186002350) at 35 °C. The mobile phase consisted of water and acetonitrile (both including 0.1% formic acid, V/V) at 0.4 mL/min. The gradient elution program was 20% B from 0 to 0.5 min, 20–50% B from 0.5 to 3 min, 50–100% B from 3.0 to 3.5 min, maintaining 100% B from 3.5 to 4.0 min, 100–20% B from 4.0 to 4.5 min, keeping 20% B from 4.5 to 5.0 min. The detection wavelength was at 315 nm.

2.9. Western blotting assays

Western blotting assays were finished based on a previous study [23,24]. In brief, the corresponding cell lysates were subjected to sodium dodecyl sulfate (SDS)-polyacrylamide gel electrophoresis, respectively. The cell lysate (40 mg total protein) was analyzed by SDS-polyacrylamide gel electrophoresis (8% acrylamide gels) and transferred onto polyvinylidene difluoride membranes (Millipore, Bedford, MA). Blots were probed with anti-UGT1A1, anti-BCRP, anti-MRP1, anti-MRP3, and anti-MRP4 followed by horseradish peroxidase-conjugated rabbit antigoat IgG (Santa Cruz Biotechnology, Santa Cruz, CA). Protein bands were detected by enhanced chemiluminescence.

2.10. Statistical analysis

All experiments were performed in triplicate. The assay data are expressed as the mean ± SD (standard deviation). Mean differences between treatment and control groups were analyzed by Student's *t*-test. The level of significance was set at $p < 0.05$ (*) or $p < 0.01$ (**) or $p < 0.001$ (***).

3. Results

3.1. Function validation of UGT1A1 enzyme in HeLa1A1 cells

In this study, to validate the function of UGT1A1 in HeLa1A1 cells, a well-accepted probe substrate of UGT1A1, β-estradiol, was applied to evaluate the glucuronidation activity [25]. Obviously, β-estradiol-3-*O*-glucuronide was produced after incubation β-estradiol with HeLa1A1 cells (Fig. 1A). In addition, β-estradiol-3-*O*-glucuronide was excreted into the

extracellular solution after incubation of β-estradiol (5 and 20 μM) with HeLa1A1 cells by a linear increase within 60 min (Fig. 1B). Moreover, the excretion rates of β-estradiol-3-*O*-glucuronide at 5 μM and 20 μM were 0.74 and 1.66 pmol/min, respectively (Fig. 1C). Taken together, these results suggested that the engineered HeLa1A1 cells could significantly express active UGT1A1 protein.

3.2. Effectiveness of Ko143 and MK571 on transporters activities

To substantiate the effectiveness of the selected inhibitors (Ko143 and MK571) on transporter activities, wushanicaritin-3-*O*-glucuronide, apigenin-7-*O*-glucuronide, chrysin-7-*O*-glucuronide and genistein-7-*O*-glucuronide were used as the model transporter substrates of BCRP, MRP1, MRP3 and MRP4, respectively [23,24,29]. Obviously, Ko143 (5 and 20 μM) led to significant reduction of excreted glucuronide (15.6%–51.7%, Fig. S1A), efflux CL_{app} value (32.3%–51.7%, Fig. S1C) and fraction metabolized (36.5%–44.1%, Fig. S1D), while a remarked increase of intracellular glucuronide (35.2%–79.7%, Fig. S1B), which kept in line with previous study [23]. In addition, similar results were observed on the excretion of apigenin-7-*O*-glucuronide (Fig. S2) [29], chrysin-7-*O*-glucuronide (Fig. S3) [24], and genistein-7-*O*-glucuronide (Fig. S4) [29] when treated with MK571 (5 and 20 μM). These results indicated that Ko143 and MK571 were effective inhibitors for BCRP and MRPs transporters, respectively.

3.3. Identification of cycloicaritin-3-O-glucuronide by HeLa1A1 cell lysate

As shown in Fig. 2A, an additional peak was obviously produced by HeLa1A1 cell lysate, whereas no metabolites were detected by wild-type HeLa cell lysate. The extracted ion chromatograms indicated that the metabolite gave a $[M + H]^+$ ion at *m/z* 545.165, which was 176.031 Da larger than that of cycloicaritin (Fig. 2B). Besides, the MS/MS analysis (Fig. 2C) also showed that HeLa1A1 cell lysate were active in the glucuronidation of cycloicaritin owing to the overexpression of UGT1A1 enzyme.

3.4. Glucuronidation assay of cycloicaritin by UGT1A1 and HeLa1A1 cell lysate

In Fig. 3, it was clear that the glucuronidation of cycloicaritin by UGT1A1 and HeLa1A1 cell lysate both followed the Hill equation. In addition, the corresponding V_{max}, n, S_{50} and CL_{max} values by UGT1A1 (Fig. 3A) were 0.54 nmol/min/mg, 1.67 μM, 1.43 μM and 0.19 mL/min/mg, respectively. Meanwhile, the V_{max}, n, S_{50} and CL_{max} values by HeLa1A1 cell lysate (Fig. 3B) were 0.04 nmol/min/mg, 1.71 μM, 1.19 μM and 0.017 mL/min/mg, respectively. Obviously, the n and S_{50} values derived with HeLa1A1 cell lysate were similar ($p > 0.05$) to the corresponding values by UGT1A1 (Fig. 3B). Moreover, since UGT1A1 enzyme was higher in recombinant materials than that in HeLa1A1 cell lysate, there were significant differences ($p < 0.001$) between the V_{max} and CL_{max} values in these two types of enzyme materials (Fig. 3B).

3.5. Chemical inhibition of cycloicaritin-3-O-glucuronidation

It is well-known that Ko143 and MK571 were specific inhibitors for BCRP and MRPs transports [23,24], while dipyridamole and LTC4 were also used to inhibit the activities of BCRP and MRPs transports [30,31]. In this study, as shown in Fig. 4, Ko143, MK571 and

dipyridamole all exhibited the dose-dependent inhibition on the glucuronidation of cycloicaritin by both UGT1A1 and HeLa1A1 cell lysate. Ko143 (20 μM), MK571 (20 μM) and dipyridamole (20 μM) displayed the potent inhibition in UGT1A1 with the remaining activity of 12.5%, 25.8% and 16.9% of the control values, respectively (Fig. 4A). Likewise, cycloicaritin-3-*O*-glucuronidation activities by HeLa1A1 cell lysate were decreased to be 8.8%, 33.3% and 14.6% of the control values in the presence of Ko143 (20 μM), MK571 (20 μM) and dipyridamole (20 μM), respectively (Fig. 4B). However, LTC4 (0.05 and 0.2 μM) did not alter the glucuronidation activity by both UGT1A1 and HeLa1A1 cell lysate (Fig. 4).

3.6. Effects of chemical inhibitors on the excretion of cycloicaritin-3-O-glucuronide

In Fig. 5A, a significant decrease (42.4%–63.8%, $p < 0.01$) in the excretion of CICT-3-G after treatment with Ko143 (5 and 20 μM). In addition, Ko143 also led to an obvious accumulation (19.7%–54.2%, $p < 0.05$) of intracellular CICT-3-G (Fig. 5B). Besides, the apparent efflux clearance (CL_{app}) of CICT-3-G was also significantly suppressed (55.4%–76.5%, $p < 0.01$) in the presence of Ko143 (Fig. 5C). It was clear that Ko143 caused obvious reductions (29.2%–32.8%, $p < 0.01$) of the fraction metabolized value (f_{met}) in cellular cycloicaritin-3-*O*-glucuronidation (Fig. 5D). Besides, dipyridamole (5 and 20 μM) caused a significant reduction (34.6%–50.0%, $p < 0.05$) in the efflux excretion (Fig. 6A) but an elevation (19.4%–37.0%, $p < 0.05$) in the intracellular level of CICT-3-G (Fig. 6B). The CL_{app} and f_{met} values were also obviously decreased (40.2%–63.5%, $p < 0.01$) and (16.0%–27.1%, $p < 0.05$), respectively (Fig. 6C and D). Because Ko143 and dipyridamole are both used as the BCRP inhibitors [24,30], these results suggested BCRP played an important role in the excretion of CICT-3-G.

It is also well-recognized that MK571 is a specific MRPs transporter inhibitors [23]. Co-incubation of MK571 (5 and 20 μM) led to a significant reduction (46.8%–64.8%, $p < 0.05$) in the efflux excretion (Fig. 7A), while the intracellular level of CICT-3-G gave an obvious elevation (50.7%–85.2%, $p < 0.01$) shown in Fig. 7B. The CL_{app} value was markedly decreased (59.7%–81.0%, $p < 0.001$, Fig. 7C), following with significant reduction of f_{met} values (15.6%–25.4%, $p < 0.05$, Fig. 7D). In addition, LTC4 also considered as a MRPs inhibitor in previous study [31]. However, LTC4 (0.05 and 0.2 μM) did not alter the rate of efflux excretion and intracellular level of CICT-3-G ($p > 0.05$, Fig. 8A and B). Meanwhile, there are no significant changes ($p > 0.05$) in either CL_{app} or f_{met} values (Fig. 8C and D).

3.7. Effects of transporters silencing on cycloicaritin-3-O-glucuronide disposition

To evaluate the role of individual efflux transporter, a series of constructed shRNA fragments (including BCRP-shRNA, MRP1-shRNA, MRP3-shRNA and MRP4-shRNA) were used to establish stable transporter knocked-down cell lines by the lentiviral transfection [23,24]. A significant decrease ($p < 0.01$) of the protein level of target transporter was observed in the corresponding stable transporter knocked-down HeLa1A1 cell lines (Fig. 9 & Table 1), which suggested that the engineered HeLa cells were successfully developed.

BCRP silencing led to an obvious reduction (26.0%–42.2%, $p < 0.01$) in the efflux excretion of CICT-3-G (Fig. 10A) but a significant elevation (32.7%, $p < 0.01$) of the intracellular

level of CICT-3-G (Fig. 10B). The BCRP-shRNA silencing resulted a marked decrease of CL_{app} value (56.5%, $p < 0.001$, Fig. 10C) as well as f_{met} value (22.5%, $p < 0.01$, Fig. 10D). The altered CICT-3-G excretion could be ascribed to the reduced expression of BCRP (Fig. 9A). These results indicated that BCRP transporter played an important role in the excretion of CICT-3-G.

Likewise, knocked-down of MRP1 transporter caused a significant decrease (23.8%–35.4%, $p < 0.05$) in the excretion of CICI-3-G (Fig. 11A) as well as the efflux clearance (52.0%, $p < 0.01$, Fig. 11C) and f_{met} values (17.0%, $p < 0.05$, Fig. 11D) of CICT-3-G. On the contrary, a marked increase (34.5%, $p < 0.05$, Fig. 11B) in the intracellular level of CICT-3-G. However, almost no changes ($p > 0.05$) in the efflux excretion (Fig. 12A), intracellular level of CICT-3-G (Fig. 12B), CL_{app} value (Fig. 12C) and f_{met} value (Fig. 12D) were observed after MRP3 silencing. In addition, silencing of MRP4 caused a moderate decrease in the excretion of CICT-3-G (11.9%–16.0%, $p < 0.05$, Fig. 13A) and in the efflux clearance (28.7%, $p < 0.05$, Fig. 13C), whereas there was a marked elevation of intracellular level of CICT-3-G (18.3%, $p < 0.05$, Fig. 13B). However, there were no significant differences ($p > 0.05$) in the f_{met} value of CICT-3-G (Fig. 13D). Taken altogether, these results indicated that the compromised CICT-3-G excretion was mainly accounted for the reduced expression of BCRP, MRP1 and MRP4 transporters.

4. Discussion

Cycloicaritin was reported with many biological properties including anti-osteoporosis effects and anti-inflammatory effects [15-18]. However, the metabolism of cycloicaritin still remain unclear so far. In previous study, icaritin and wushanicaritin, two cycloicaritin derivatives, have been proved to undergo massive glucuronidation in human liver ($CL_{int} > 0.35$ mL/min/mg) and human intestine ($CL_{int} > 0.18$ mL/min/mg) [25,26]. Likewise, cycloicaritin also could be efficiently metabolized to cycloicaritin-3-*O*-glucuronide by UGT1A1 enzyme with the CL_{int} value of 0.19 mL/min/mg (Fig. 3A) in this study. These findings suggested that the pharmacokinetics and oral bioavailability of cycloicaritin would be influenced by hepatic and intestinal first-pass glucuronidation because UGT1A1 was expressed in human liver and intestine [2]. Therefore, the role of cycloicaritin-3-*O*-glucuronidation in determining the oral bioavailability should not be underestimated.

Since bovine serum albumin (BSA) effect on the glucuronidation would greatly influence the *in vitro* activity by human liver microsomes or recombinant enzyme, it is incorrect using CL_{int} ($= V_{max}/K_m$) value to test the glucuronidation capability [32]. There is general agreement on the need to correct kinetic constants including K_m and K_i, values for the fraction of unbound drug concentration (*fu*) to ensure optimal prediction of clearance and inhibition potential *in vivo* from *in vitro* hepatic microsomal studies [33]. In this study, according to the Hallifax and Houston model [33], we can speculate that the binding of cycloicaritin (logP = 2.2) and UGT1A1 protein was $fu > 0.99$, which the BSA effect could be negligible. Hence, the kinetic parameters by UGT1A1 were not corrected according to the protein binding rate (Fig. 3A). Besides, CL_{int} ($= V_{max}/K_m$) value was used to evaluate the catalytic efficiency of the enzyme because CL_{int} value is independent of the substrate concentration and more relevant in an attempt to predict the clearance *in vivo* [34].

Traditionally, three of the most common and popular cell lines used to evaluate the efflux excretion of metabolites in epithelial cells are Caco-2, Madin-Darby canine kidney II (MDCK-II) and HeLa cell lines [24,35,36]. However, Caco-2 and MDCK-II cell models are still too complex to delineate the roles of efflux transporters, because massive other phase II enzymes (e.g., sulfotransferase) are also expressed in these two cells [28]. Therefore, we modified the HeLa cells to develop an engineered cell model to study the roles of transporters in the excretion of glucuronide. There are three advantages for the use of HeLa1A1 cells [37]. First, we can ignore the elimination of cycloicaritin since rare endogenous drug metabolizing enzymes were expressed in HeLa cells. Second, an array of transporters including BCRP, MRP1, MRP3 and MRP4 were significantly expressed in HeLa cells [29], which was a closer mimic of the *in vivo* situations. Third, HeLa cells, as engineered cells, can easily be transiently or stably transfected with an uptake or efflux transporter, or individual enzyme interested [24,28].

To date, numerous researches reported that Ko143 and MK571 both could obviously inhibit the excretion of several flavonoid-related glucuronides [23,24,36,37]. In this study, use of Ko143 and MK571 also can bring a significant reduction in the excretion rates and efflux clearance (Figs. 5 and 7). However, identification of efflux transporters responsible for glucuronide excretion by chemical inhibitors should be treated with caution due to their potential in modification of the glucuronidation activity. Because Ko143 and MK571 both exhibited obvious concentration-dependent inhibitory effects on cycloicaritin-3-*O*-glucuronidation by UGT1A1 (Fig. 4A) and HeLa1A1 cell lysate (Fig. 4B), thus, the altered glucuronide excretion could be attributed to a reduced BCRP activity by chemical inhibitors or suppressed metabolism by UGT1A1 in HeLa1A1 cells. In addition, dipyridamole also reduced the efflux clearance of cycloicaritin-3-*O*-glucuronide (Fig. 6), although it is not a specific inhibitor of BCRP. Likewise, LTC4, a high-affinity substrate of MRP1/MRP2, did not alter the efflux excretion of cycloicaritin-3-*O*-glucuronide (Fig. 8). So far, dipyridamole and LTC4 have not gained the widespread use as the inhibitors of BCRP and MRPs transporters [30,31]. The reason could be that little is known about their inhibitory effects toward other transporters.

Moreover, decreased protein expression using shRNA mediated gene silencing technique was widely applied to determine the role of efflux transporters in glucuronide excretion [23,24,29,37]. In fact, partial silencing of BCRP and MRPs led to significant changes in cycloicaritin-3-*O*-glucuronide excretion and intracellular accumulation (Figs. 10, 11 and 13), confirming that BCRP, MRP1 and MPR4 all played a major contribution to glucuronide transport. These findings were in line with the excretion results of wushanicaritin glucuronides [23]. Meanwhile, introduction of shRNA of MRP3 did not alter glucuronide transport or cellular accumulation (Fig. 12). Not surprisingly, there is an important limitation for the capability of MRP2 in this study due to the absence of MRP2 in HeLa cells [38]. Previous studies have proved that MRP2 displayed significant roles in the flavonoid glucuronide transport [39,40]. As for the role of MRP2 in cycloicaritin-3-*O*-glucuronide transport, we would perform the experiments using MDCK cells or HEK293 cells in future [38].

5. Conclusion

In this study, the engineered HeLa cells which are stably transfected with UGT1A1 (named HeLa1A1 cells) are a simple and appropriate tool to study the excretion of cycloicaritin-3-*O*-glucuronide. HeLa1A1 cells could express UGT1A1 protein and catalyze the cycloicaritin-3-*O*-glucuronidation. In addition, Ko143 and MK571 led to a significant reduction of cellular excretion of the glucuronide. Remarkably, the presence of MRP3 did not significantly alter the major efflux mechanism for cycloicaritin-3-*O*-glucuronide, which remains to be BCRP, MRP1 and MRP4. Further, BCRP played a critical role in the disposition of cycloicaritin-3-*O*-glucuronide, whereas the contribution of MRP1 and MRP4 were moderate. Rapid glucuronidation metabolism by UGT1A1 and efflux transport through BCRP, MRP1 and MRP4 would play an important role in the low bioavailability of cycloicaritin. Taken together, this study established an UGT1A1-overexpressing HeLa cells which were a useful tool for studying UGT1A1 functions at a cellular level.

Supplementary Material

Refer to Web version on PubMed Central for supplementary material.

Acknowledgements

This work was financially supported by the Program of Introducing Talents of Discipline to Universities (No. B13038), Major Project for International Cooperation and Exchange of the National Natural Science Foundation of China (No. 81220108028), Guangdong Provincial Science and Technology Project (No. 2016B090921005), State Key Program of National Natural Science Foundation of China (81630097) and National Natural Science Foundation of Guangdong (2017A03031387).

References

[1]. Williams JA, Hyland R, Jones BC, Smith DA, Hurst S, Goosen TC, Peterkin V, Koup JR, Ball SE, Drug-drug interactions for UDP-glucuronosyltransferase substrates: a pharmacokinetic explanation for typically observed low exposure (AUCi/AUC) ratios, Drug Metab. Dispos. 32 (2004) 1201–1208. [PubMed: 15304429]

[2]. Uchaipichat V, Mackenzie PI, Elliot DJ, Miners JO, Selectivity of substrate (trifluoperazine) and inhibitor (amitriptyline, androsterone, canrenoic acid, hecogenin, phenylbutazone, quinidine, quinine, and sulfinpyrazone) "probes" for human udp-glucuronosyltransferases, Drug Metab. Dispos. 34 (2006) 449–456. [PubMed: 16381668]

[3]. Evans WE, Relling MV, Pharmacogenomics: translating functional genomics into rational therapeutics, Science 286 (1999) 487–491. [PubMed: 10521338]

[4]. Wienkers LC, Heath TG, Predicting in vivo drug interactions from in vitro drug discovery data, Nature reviews, Drug Discov 4 (2005) 825–833.

[5]. Yang N, Sun R, Liao X, Aa J, Wang G, UDP-glucuronosyltransferases (UGTs) and their related metabolic cross-talk with internal homeostasis: a systematic review of UGT isoforms for precision medicine, Pharmacol. Res. 121 (2017) 169–183. [PubMed: 28479371]

[6]. Sugatani J, Function, genetic polymorphism, and transcriptional regulation of human UDP-glucuronosyltransferase (UGT) 1A1, Drug Metabol. Pharmacokinet. 28 (2013) 83–92.

[7]. Wu B, Jiang W, Yin T, Gao S, Hu M, A new strategy to rapidly evaluate kinetics of glucuronide efflux by breast cancer resistance protein (BCRP/ABCG2), Pharm. Res. 29 (2012) 3199–3208. [PubMed: 22752253]

[8]. Stieger B, Meier PJ, Pharmacogenetics of drug transporters in the enterohepatic circulation, Pharmacogenomics 12 (2011) 611–631. [PubMed: 21619426]

[9]. Higgins CF, ABC transporters: physiology, structure and mechanism-an overview, Res. Microbiol. 152 (2001) 205–210. [PubMed: 11421269]

[10]. Yang X, Gandhi YA, Duignan DB, Morris ME, Prediction of biliary excretion in rats and humans using molecular weight and quantitative structure-pharmacokinetic relationships, AAPS J. 11 (2009) 511–525. [PubMed: 19593675]

[11]. Ge S, Gao S, Yin T, Hu M, Determination of pharmacokinetics of chrysin and its conjugates in wild-type FVB and Bcrpl knockout mice using a validated LC-MS/MS method, J. Agric. Food Chem. 63 (2015) 2902–2910. [PubMed: 25715997]

[12]. Ge S, Yin T, Xu B, Gao S, Hu M, Curcumin affects phase II disposition of resveratrol through inhibiting efflux transporters MRP2 and BCRP, Pharm. Res. (N. Y.) 33 (2016) 590–602.

[13]. Zheng L, Zhu L, Zhao M, Shi J, Li Y, Yu J, Jiang H, Wu J, Tong Y, Liu Y, Hu M, Lu L, Liu Z, In vivo exposure of kaempferol is driven by phase II metabolic enzymes and efflux transporters, AAPS J. 18 (2016) 1289–1299. [PubMed: 27393480]

[14]. Dell'Agli M, Galli G, Cero ED, Belluti F, Matera R, Zironi E, Pagliuca G, Bosisio E, Potent inhibition of human phosphodiesterase-5 by icariin derivatives, J. Nat. Prod. 71 (2008) 1513–1517. [PubMed: 18778098]

[15]. Zheng ZG, Zhou YP, Zhang X, Thu PM, Xie ZS, Lu C, Pang T. Xue B, Xu DQ, Chen Y, Chen XW, Li HJ, Xu X, Anhydroicaritin improves diet-induced obesity and hyperlipidemia and alleviates insulin resistance by suppressing SREBPs activation, Biochem. Pharmacol. 122 (2016) 42–61. [PubMed: 27816546]

[16]. Chen S-R, Xu X-Z, Wang Y-H, Chen J-W, Xu S-W, Gu L-Q, Liu P-Q, Icariin derivative inhibits inflammation through suppression of p38 mitogen-activated protein kinase and nuclear factor-kappaB pathways, Biol. Pharm. Bull. 33 (2010) 1307–1313. [PubMed: 20686223]

[17]. Tantry MA, Dar JA, Idris A, Akbar S, Shawl AS, Acylated flavonol glycosides from Epimedium elatum, a plant endemic to the Western Himalayas, Fitoterapia 83 (2012) 665–670. [PubMed: 22366553]

[18]. Liu DF, Li YP, Ou TM, Huang SL, Gu LQ, Huang M, Huang ZS, Synthesis and antimultidrug resistance evaluation of icariin and its derivatives, Bioorg. Med. Chem. Lett 19 (2009) 4237–4240. [PubMed: 19523827]

[19]. Jiang J, Li J, Zhang Z, Sun E, Feng L, Jia X, Mechanism of enhanced antiosteoporosis effect of circinal-icaritin by self-assembled nanomicelles in vivo with suet oil and sodium deoxycholate, Int. J. Nanomed 10 (2015) 2377–2389.

[20]. Wu B, Pharmacokinetic interplay of phase II metabolism and transport: a theoretical study, J. Pharmacol. Sci 101 (2012) 381–393.

[21]. Dai P, Zhu L, Luo F, Lu L, Li Q, Wang L, Wang Y, Wang X, Hu M, Liu Z, Triple recycling processes impact systemic and local bioavailability of orally administered flavonoids, AAPS J. 17 (2015) 723–736. [PubMed: 25762448]

[22]. Geng JL, Dai Y, Yao ZH, Qin ZF, Wang XL, Qin L, Yao XS, Metabolites profile of Xian-Ling-Gu-Bao capsule, a traditional Chinese medicine prescription, in rats by ultra performance liquid chromatography coupled with quadrupole time-of-flight tandem mass spectrometry analysis, J. Pharmaceut. Biomed. Anal. 96 (2014) 90–103.

[23]. Qin Z, Li S, Yao Z, Hong X, Wu B, Krausz KW, Gonzalez FJ, Gao H, Yao X, Chemical inhibition and stable knock-down of efflux transporters leads to reduced glucuronidation of wushanicaritin in UGT1A1-overexpressing HeLa cells: the role of breast cancer resistance protein (BCRP) and multidrug resistance-associated proteins (MRPs) in the excretion of glucuronides, Food Funct 9 (2018) 1410–1423. [PubMed: 29318243]

[24]. Quan E, Wang H, Dong D, Zhang X, Wu B, Characterization of chrysin glucuronidation in UGT1A1-overexpressing HeLa cells: elucidating the transporters responsible for efflux of glucuronide, Drug Metab. Dispos. 43 (2015) 433–443. [PubMed: 25595598]

[25]. Hong X, Zheng Y, Qin Z, Wu B, Dai Y, Gao H, Yao Z, Gonzalez FJ, Yao X, In vitro glucuronidation of wushanicaritin by liver microsomes, intestine microsomes and expressed human UDP-glucuronosyltransferase enzymes, Int. J. Mol. Sci. 18 (2017) 1983.

[26]. Wang L, Hong X, Yao Z, Dai Y, Zhao G, Qin Z, Wu B, Gonzalez FJ, Yao X, Glucuronidation of icaritin by human liver microsomes, human intestine microsomes and expressed UDP-

glucuronosyltransferase enzymes: identification of UGT1A3, 1A9 and 2B7 as the main contributing enzymes, Xenobiotica 48 (2018) 357–367. [PubMed: 28443723]

[27]. Hutzler JM, Tracy TS, Atypical kinetic profiles in drug metabolism reactions, Drug Metab. Dispos. 30 (2002) 355–362. [PubMed: 11901086]

[28]. Jiang W, Xu B, Wu B, Yu R, Hu M, UDP-glucuronosyltransferase (UGT) 1A9-overexpressing HeLa cells is an appropriate tool to delineate the kinetic interplay between breast cancer resistance protein (BRCP) and UGT and to rapidly identify the glucuronide substrates of BCRP, Drug Metab. Dispos. 40 (2012) 336–345. [PubMed: 22071170]

[29]. Zhang X, Dong D, Wang H, Ma Z, Wang Y, Wu B, Stable knock-down of efflux transporters leads to reduced glucuronidation in UGT1A1-overexpressing HeLa cells: the evidence for glucuronidation-transport interplay, Mol. Pharm. 12 (2015) 1268–1278. [PubMed: 25741749]

[30]. Zhang Y, Gupta A, Wang H, Zhou L, Vethanayagam RR, Unadkat JD, Mao Q, BCRP transports dipyridamole and is inhibited by calcium channel blockers, Pharm. Res. 22 (2005) 2023–2034. [PubMed: 16247709]

[31]. Loe DW, Almquist KC, Deeley RG, Cole SP, Multidrug resistance protein (MRP)-mediated transport of leukotriene C4 and chemotherapeutic agents in membrane vesicles. Demonstration of glutathione-dependent vincristine transport, J. Biol. Chem. 271 (1996) 9675–9682. [PubMed: 8621643]

[32]. Manevski N, Moreolo PS, Yli-Kauhaluoma J, Finel M, Bovine serum albumin decreases Km values of human UDP-glucuronosyltransferases 1A9 and 2B7 and increases Vmax values of UGT1A9, Drug Metab. Dispos. 39 (2011) 2117–2129. [PubMed: 21856742]

[33]. Hallifax D, Houston JB, Binding of drugs to hepatic microsomes: comment and assessment of current prediction methodology with recommendation for improvement, Drug Metab. Dispos. 34 (2006) 724–726. [PubMed: 16552024]

[34]. Wu B, Dong D, Hu M, Zhang S, Quantitative prediction of glucuronidation in humans using the in vitro-in vivo extrapolation approach, Curr. Top. Med. Chem. 13 (2013) 1343–1352. [PubMed: 23675940]

[35]. Dai P, Zhu L, Yang X, Zhao M, Shi J, Wang Y, Lu L, Liu Z, Multidrug resistance-associated protein 2 is involved in the efflux of Aconitum alkaloids determined by MRP2-MDCKII cells, Life Sci. 127 (2015) 66–72. [PubMed: 25744397]

[36]. Ye L, Yang X, Yang Z, Gao S, Yin T, Liu W, Wang F, Hu M, Liu Z, The role of efflux transporters on the transport of highly toxic aconitine, mesaconitine, hypaconitine, and their hydrolysates, as determined in cultured Caco-2 and transfected MDCKII cells, Toxicol. Lett. 216 (2013) 86–99. [PubMed: 23200901]

[37]. Sun H, Zhou X, Zhang X, Wu B, Decreased expression of multidrug resistance-associated protein 4 (MRP4/ABCC4) leads to reduced glucuronidation of flavonoids in UGT1A1-overexpressing HeLa cells: the role of futile recycling, J. Agric. Food Chem. 63 (2015) 6001–6008. [PubMed: 26066637]

[38]. Ahlin G, Hilgendorf C, Karlsson J, Szigyarto CA, Uhlen M, Artursson P, Endogenous gene and protein expression of drug-transporting proteins in cell lines routinely used in drug discovery programs, Drug Metab. Dispos. 37 (2009) 2275–2283. [PubMed: 19741037]

[39]. Wang M, Yang G, He Y, Xu B, Zeng M, Ge S, Yin T, Gao S, Hu M, Establishment and use of new MDCK II cells overexpressing both UGT1A1 and MRP2 to characterize flavonoid metabolism via the glucuronidation pathway, Mol. Nutr. Food Res. 60 (2016) 1967–1983. [PubMed: 26833852]

[40]. Williamson G, Aeberli I, Miguet L, Zhang Z, Sanchez MB, Crespy V, Barron D, Needs P, Kroon PA, Glavinas H, Krajcsi P, Grigorov M, Interaction of positional isomers of quercetin glucuronides with the transporter ABCC2 (cMOAT, MRP2), Drug Metab. Dispos. 35 (2007) 1262–1268. [PubMed: 17478601]

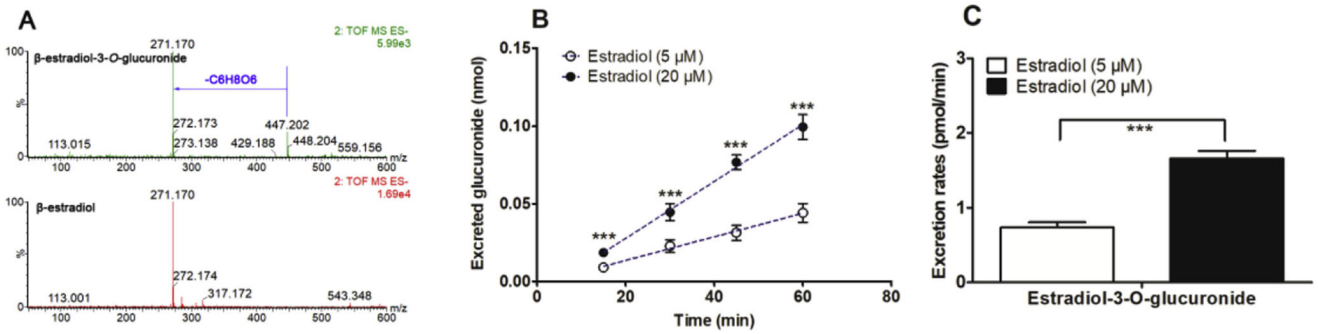

Fig. 1. ESI-MS/MS spectra of β-estradiol and β-estradiol-S-*O*-glucuronide, and UGT1A1-mediated β-estradiol-*O*-glucuronidation in HeLa1A1 cells.

(A) ESI-MS/MS spectra of β-estradiol and β-estradiol-3-*O*-glucuronide in negative ion mode; (B) Excreted β-estradiol-3-*O*-glucuronide in extracellular solution at two concentrations of propofol (5 and 20 μM); (C) Excreted rates of β-estradiol-3-*O*-glucuronide at different concentrations (5 and 20 μM); Data were presented as mean ± SD. *$p < 0.05$, **$p < 0.01$ or ***$p < 0.001$ compared with that of β-estradiol (5 μM).

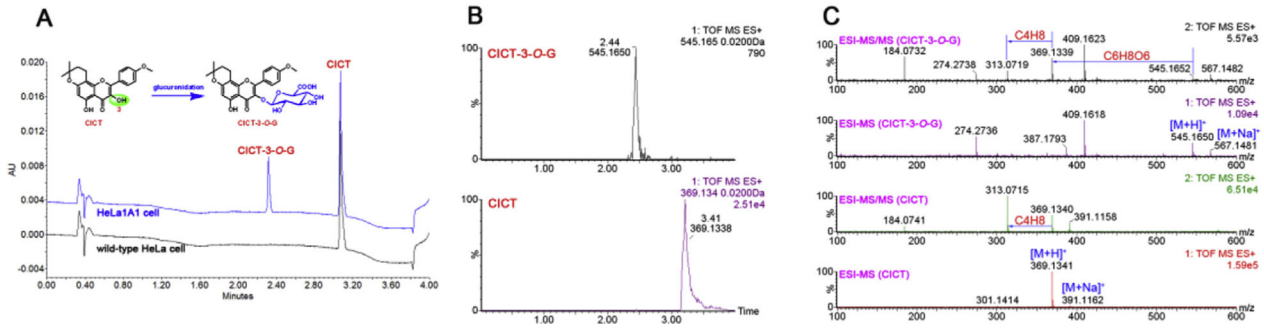

Fig. 2. Representative UPLC chromatograms, extracted ion chromatograms, MS/MS spectra of cycloicaritin and cycloicaritin-3-*O*-glucuronide.

(A) UPLC chromatograms of CICT and CICT-3-G after incubation with HeLa1A1 cell lysate and cycloicaritin (8 μM) for 2 h. (B) Extracted ion chromatograms of CICT (*m/z* 369.1338) and CICT-3-G (*m/z* 545.1650) in positive ion mode. (C) The MS and MS/MS spectra of CICT and CICT-3-G in positive ion mode.

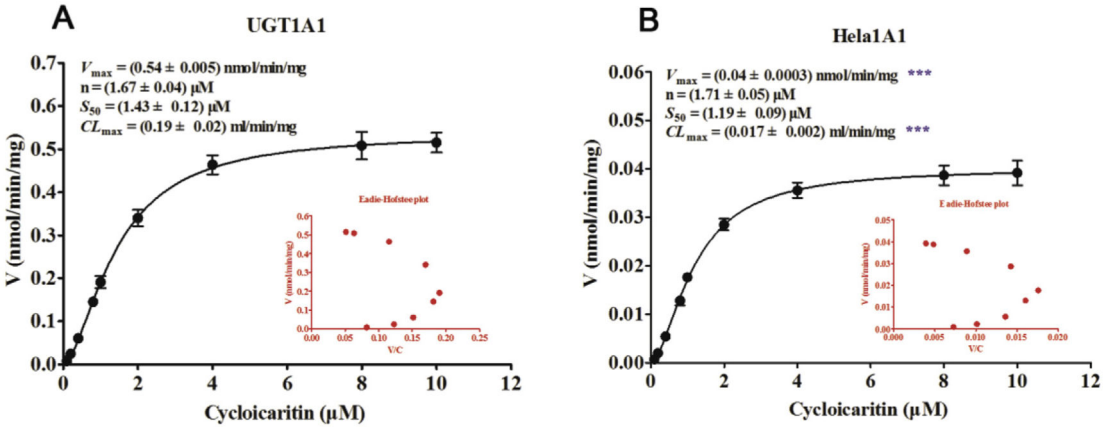

Fig. 3. Kinetic profiles for cycloicaritin-3-*O*-glucuronidation by recombinant UGT1A1 enzyme and HeLa1A1 cell lysate.

(A) Kinetic profile for cycloicaritin-3-*O*-glucuronidation by expressed UGT1A1. (B) Kinetic profile for cycloicaritin-3-*O*-glucuronidation by HeLa1A1 cell lysate. In each panel, the insert figure showed the corresponding Eadie-Hofstee plot. Each data point was the average of three determinations with the error bar representing the S.D. (n = 3). (* Parameters were compared with the same parameters of CICT-3-G by UGT1A1, ***$p < 0.001$).

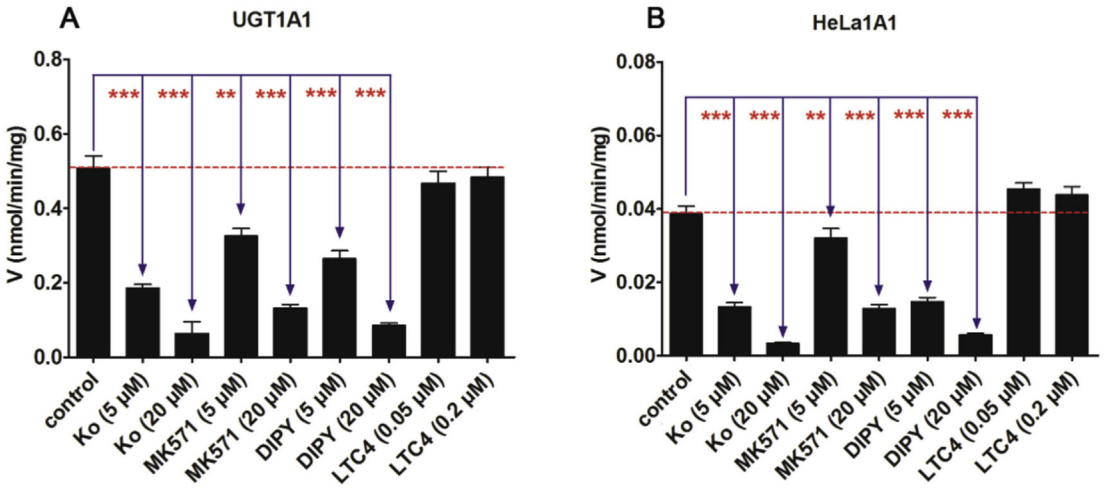

Fig. 4. Effects of chemical inhibitors (Ko143, MK-571, dipyridamole and LTC4) on cycloicaritin-3-*O*-glucuronidation by expressed UGT1A1 and HeLa1A1 cell lysate.

The concentration of cycloicaritin was 8 μM. (A) Effects of chemical inhibitors for CICT-3-G by recombinant UGT1A1. (B) Effects of chemical inhibitors for CICT-3-G by HeLa1A1 cell lysate. DIPY, dipyridamole; LTC4, leukotriene C4; CICT-3-G, cycloicaritin-3-*O*-glucuronide; All experiments were performed in triplicate (n = 3). (* Compared with the values of control, *$p < 0.05$, **$p < 0.01$, ***$p < 0.001$).

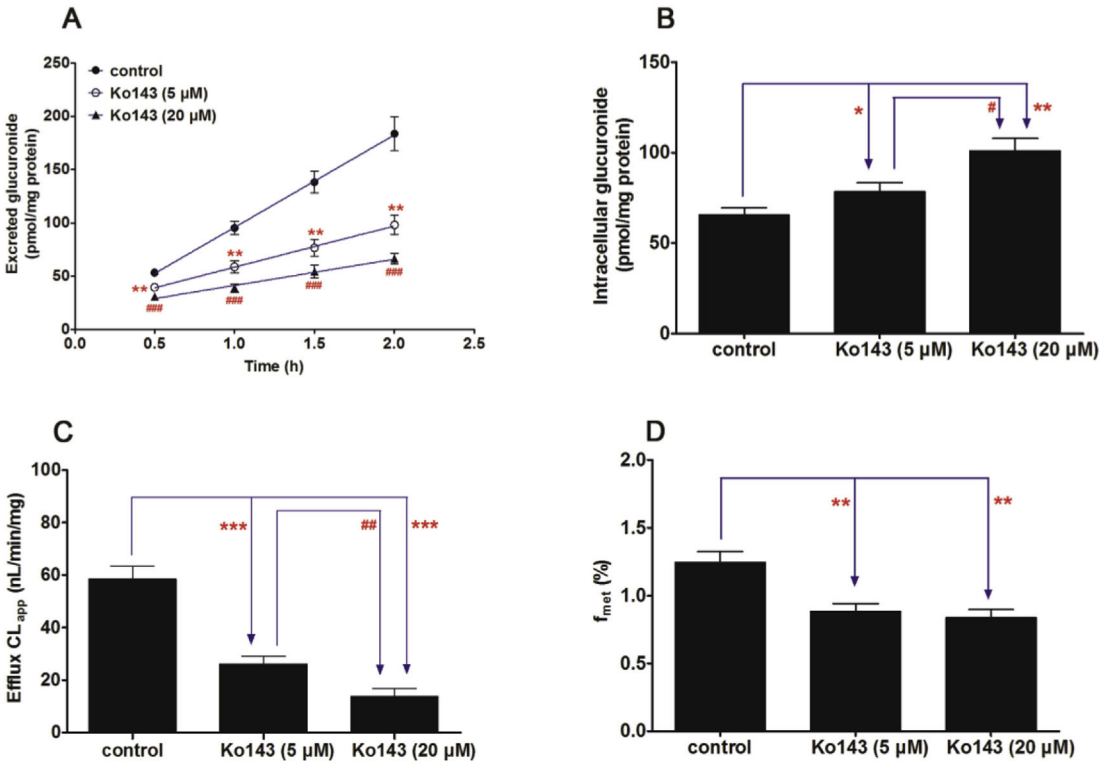

Fig. 5. Effects of Ko143 (5 and 20 μM) on the cycloicaritin-3-*O*-glucuronidation after incubation with cycloicaritin in HeLa1A1 cells.

(A) Effects of Ko143 on the excretion rates of CICT-3-G; (B) Effects of Ko143 on the intracellular levels of CICT-3-G; (C) Effects of Ko143 on the efflux clearances ($CL_{ef,app}$) of CICT-3-G; (D) Effects of Ko143 on the fraction metabolized (f_{met}) value of CICT-3-G. CICT-3-G, cycloicaritin-3-*O*-glucuronide. All experiments were performed in triplicate (n = 3). [* Parameters of CICT-3-G in Ko143 (5 and 20 μM) treated HeLa1A1 cells group were compared with the same parameters of CICT-3-G in control group, $^{*}p < 0.05$, $^{**}p < 0.01$, $^{***}p < 0.001$; $^{\#}$ Parameters of CICT-3-G in Ko143 (5 μM) treated HeLa1A1 cells group were compared with the same parameters of CICT-3-G in Ko143 (20 μM) treated HeLa1A1 cells group, $^{\#}p < 0.05$, $^{\#\#}p < 0.01$, $^{\#\#\#}p < 0.001$].

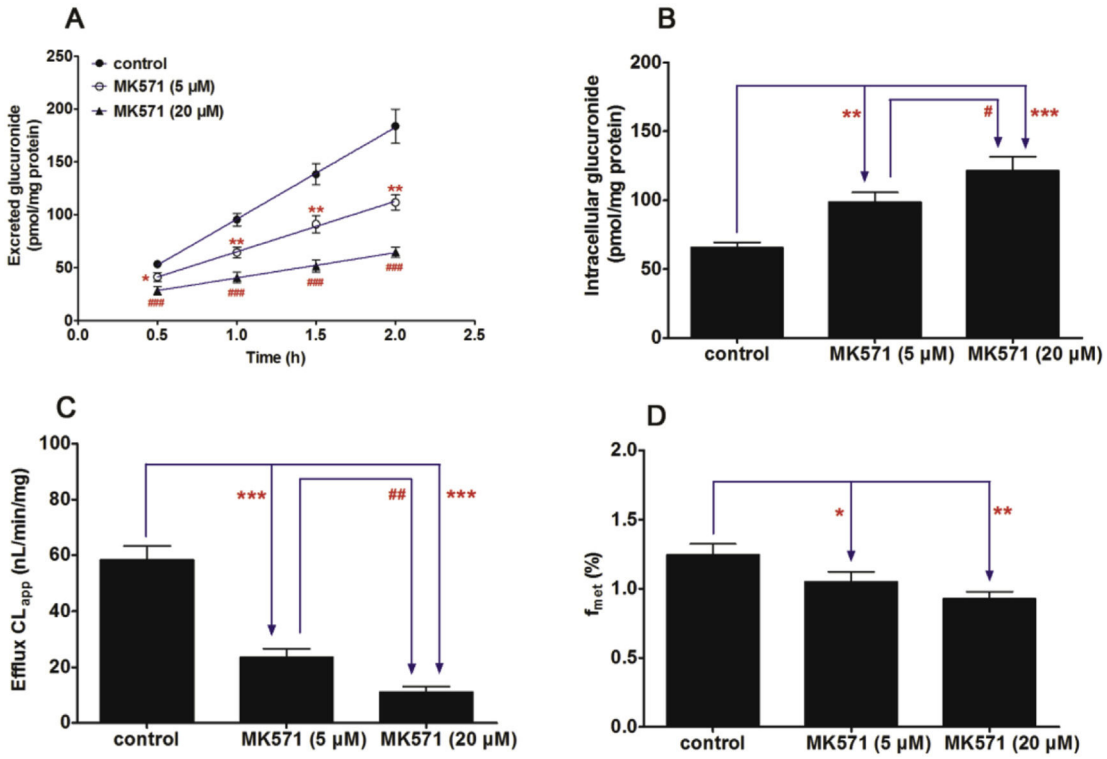

Fig. 6. Effects of MK571 (5 and 20 μM) on the cycloicaritin-3-*O*-glucuronidation after incubation with cycloicaritin in HeLa1A1 cells.

(A) Effects of MK571 on the excretion rates of CICT-3-G; (B) Effects of MK571 on the intracellular levels of CICT-3-G; (C) Effects of MK571 on the efflux clearances ($CL_{ef,app}$) of CICT-3-G; (D) Effects of MK571 on the fraction metabolized (f_{met}) value of CICT-3-G. CICT-3-G, cycloicaritin-3-*O*-glucuronide. All experiments were performed in triplicate (n = 3). [* Parameters of CICT-3-G in MK571 (5 and 20 μM) treated HeLa1A1 cells group were compared with the same parameters of CICT-3-G in control group, *$p < 0.05$, **$p < 0.01$, ***$p < 0.001$; # Parameters of CICT-3-G in MK571 (5 μM) treated HeLa1A1 cells group were compared with the same parameters of CICT-3-G in MK571 (20 μM) treated HeLa1A1 cells group, *$p < 0.05$, **$p < 0.01$, ***$p < 0.001$].

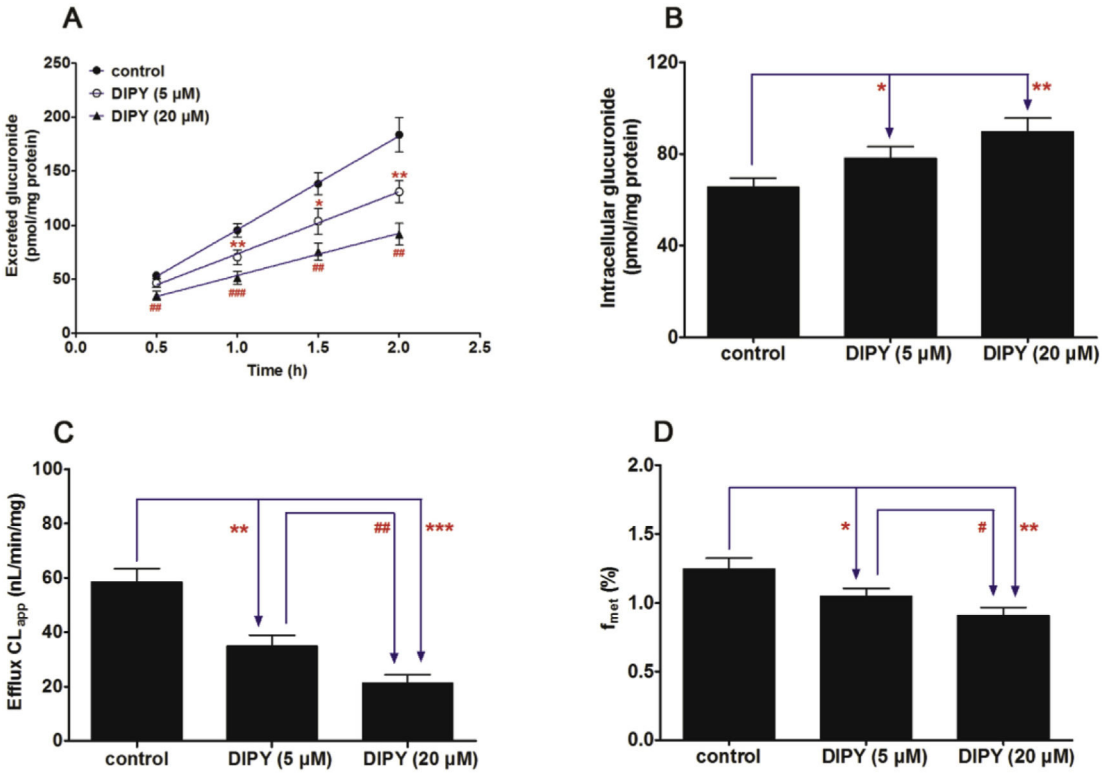

Fig. 7. Effects of dipyridamole (5 and 20 μM) on the cycloicaritin-3-*O*-glucuronidation after incubation with cycloicaritin in HeLa1A1 cells.

(A) Effects of DIPY on the excretion rates of CICT-3-G; (B) Effects of DIPY on the intracellular levels of CICT-3-G; (C) Effects of DIPY on the efflux clearances ($CL_{ef,app}$) of CICT-3-G; (D) Effects of DIPY on the fraction metabolized (f_{met}) value of CICT-3-G. CICT-3-G, cycloicaritin-3-*O*-glucuronide. All experiments were performed in triplicate (n = 3). DIPY, dipyridamole. [* Parameters of CICT-3-G in DIPY (5 and 20 μM) treated HeLa1A1 cells group were compared with the same parameters of CICT-3-G in control group, $^{*}p < 0.05$, $^{**}p < 0.01$, $^{***}p < 0.001$; $^{\#}$ Parameters of CICT-3-G in DIPY (5 μM) treated HeLa1A1 cells group were compared with the same parameters of CICT-3-G in DIPY (20 μM) treated HeLa1A1 cells group, $^{\#}p < 0.05$, $^{\#\#}p < 0.01$, $^{\#\#\#}p < 0.001$].

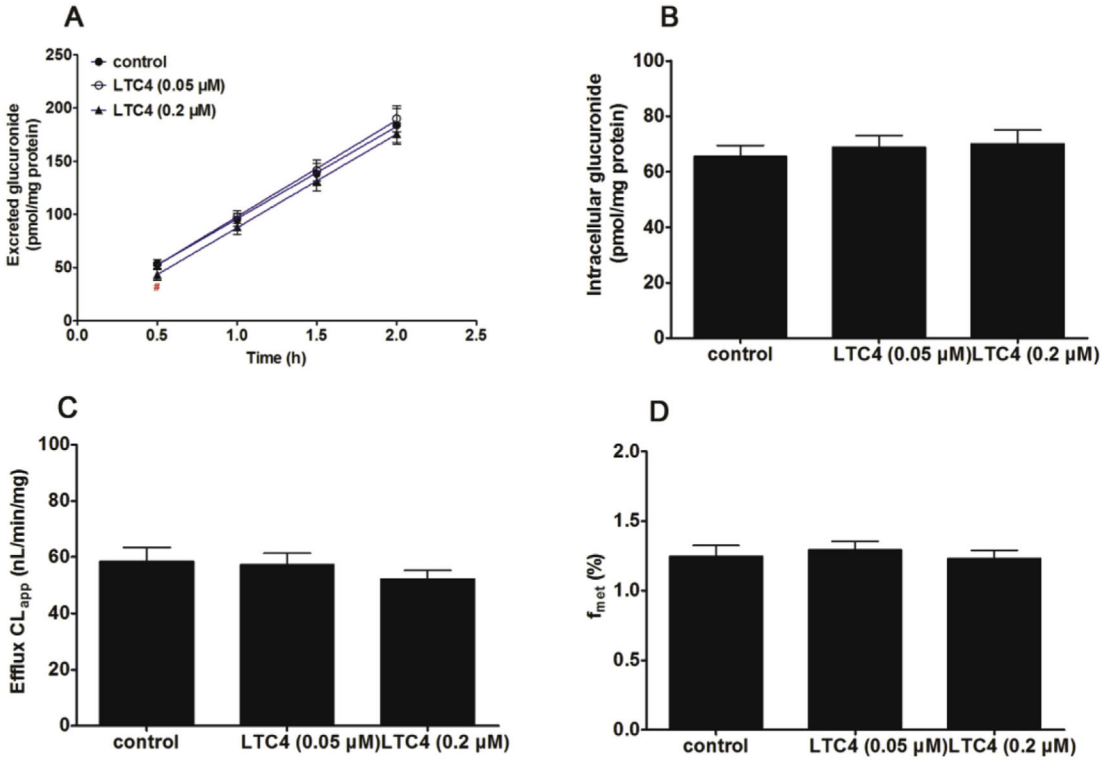

Fig. 8. Effects of LTC4 (0.05 and 0.2 μM) on the cycloicaritin-3-*O*-glucuronidation after incubation with cycloicaritin in HeLa1A1 cells.

(A) Effects of LTC4 on the excretion rates of CICT-3-G; (B) Effects of LTC4 on the intracellular levels of CICT-3-G; (C) Effects of LTC4 on the efflux clearances ($CL_{ef,app}$) of CICT-3-G; (D) Effects of LTC4 on the fraction metabolized (f_{met}) value of CICT-3-G. CICT-3-G, cycloicaritin-3-*O*-glucuronide. All experiments were performed in triplicate (n = 3). LTC4, leukotriene C4. [* Parameters of CICT-3-G in LTC4 (0.05 and 0.2 μM) treated HeLa1A1 cells group were compared with the same parameters of CICT-3-G in control group, $^{*}p < 0.05$, $^{**}p < 0.01$, $^{***}p < 0.001$; # Parameters of CICT-3-G in LTC4 (0.05 μM) treated HeLa1A1 cells group were compared with the same parameters of CICT-3-G in LTC4 (0.2 μM) treated HeLa1A1 cells group, $^{\#}p < 0.05$, $^{\#\#}p < 0.01$, $^{\#\#\#}p < 0.001$].

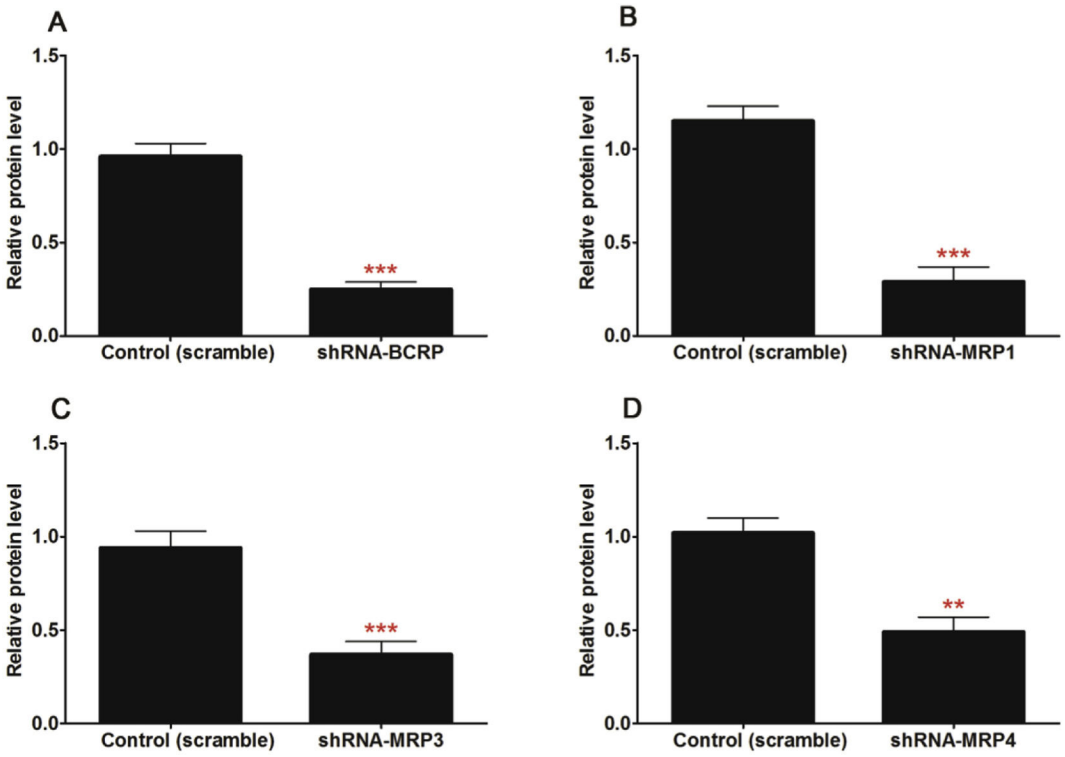

Fig. 9. Relative protein expression of transporters (normalized to the levels of GAPDH) in HeLa1A1 and engineered HeLa1A1 cells based on western blotting.

(A) Effects of gene silencing on the protein level of BCRP. (B) Effects of gene silencing on the protein level of MRP1. (C) Effects of gene silencing on the protein level of MRP3. (D) Effects of gene silencing on the protein level of MRP4. All experiments were performed in triplicate (n = 3). (* protein levels of corresponding efflux transports in engineered HeLa1A1 cells were compared with these in control HeLa1A1 cells. *$p < 0.05$, **$p < 0.01$, ***$p < 0.001$).

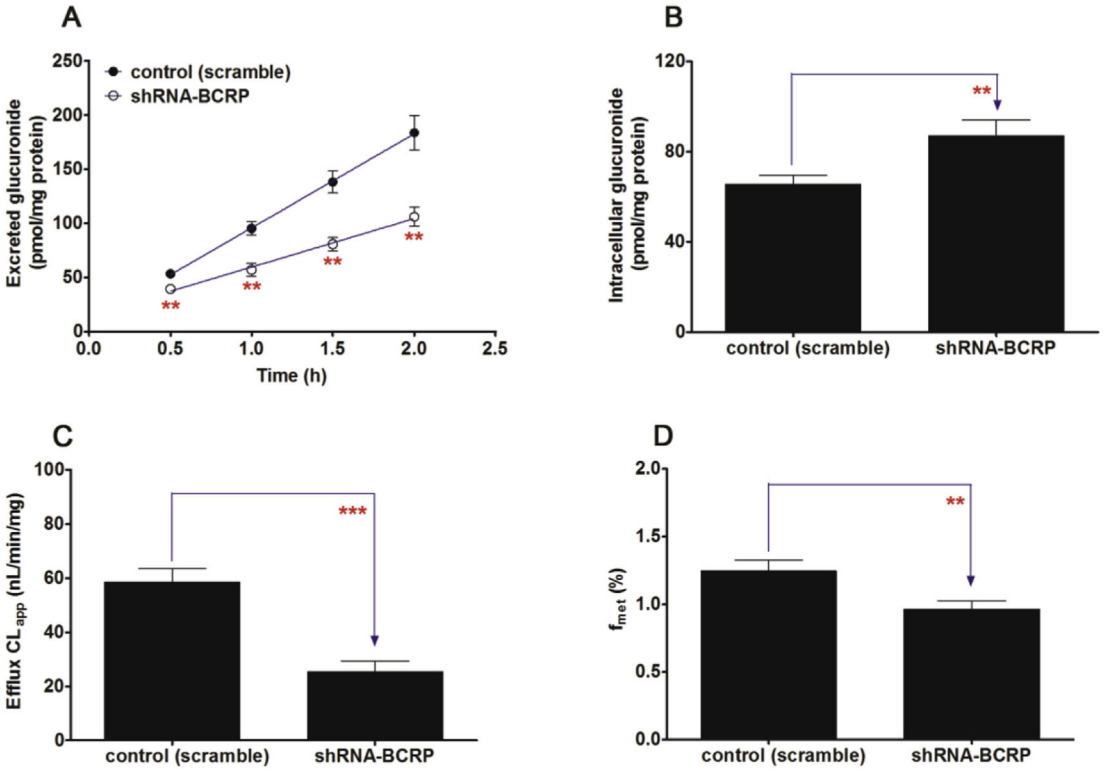

Fig. 10. Effects of BCRP silencing on the excretion of cycloicaritin-3-*O*-glucuronide and cellular glucuronidation.

(A) Effects of BCRP silencing on the excretion rates of CICT-3-G; (B) Effects of BCRP silencing on the intracellular levels of CICT-3-G; (C) Effects of BCRP silencing on the efflux clearances ($CL_{ef,app}$) of CICT-3-G; (D) Effects of MRP3 silencing on cellular glucuronidation (or f_{met}) of CICT-3-G. CICT-3-G, cycloicaritin-3-*O*-glucuronide; All experiments were performed in triplicate (n = 3). (* Parameters of CICT-3-G in engineered HeLa1A1 cells were compared with the same parameters in control group, $*p < 0.05$, $**p < 0.01$, $***p < 0.001$).

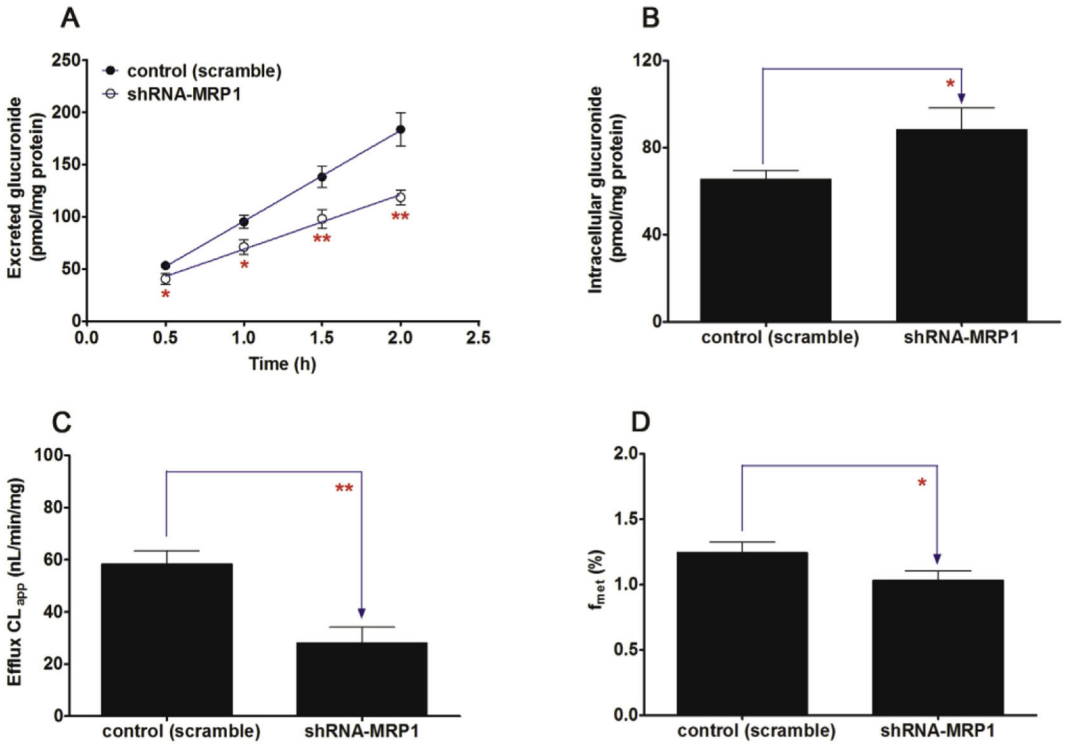

Fig. 11. Effects of shRNA-mediated MRP1 knock-down on the excretion of cycloicaritin-3-*O*-glucuronide and cellular glucuronidation.

(A) Effects of MRP1 knock-down on the excretion rates of CICT-3-G; (B) Effects of MRP1 knock-down on the intracellular levels of CICT-3-G; (C) Effects of MRP1 knock-down on the efflux clearances ($CL_{ef,app}$) of CICT-3-G; (D) Effects of MRP1 knock-down on cellular glucuronidation (or f_{met}) of CICT-3-G; CICT-3-G, cycloicaritin-3-*O*-glucuronide; (* Parameters of CICT-3-G in engineered HeLa1A1 cells were compared with the same parameters in control group, $*p < 0.05$, $**p < 0.01$, $***p < 0.001$). All experiments were performed in triplicate (n = 3).

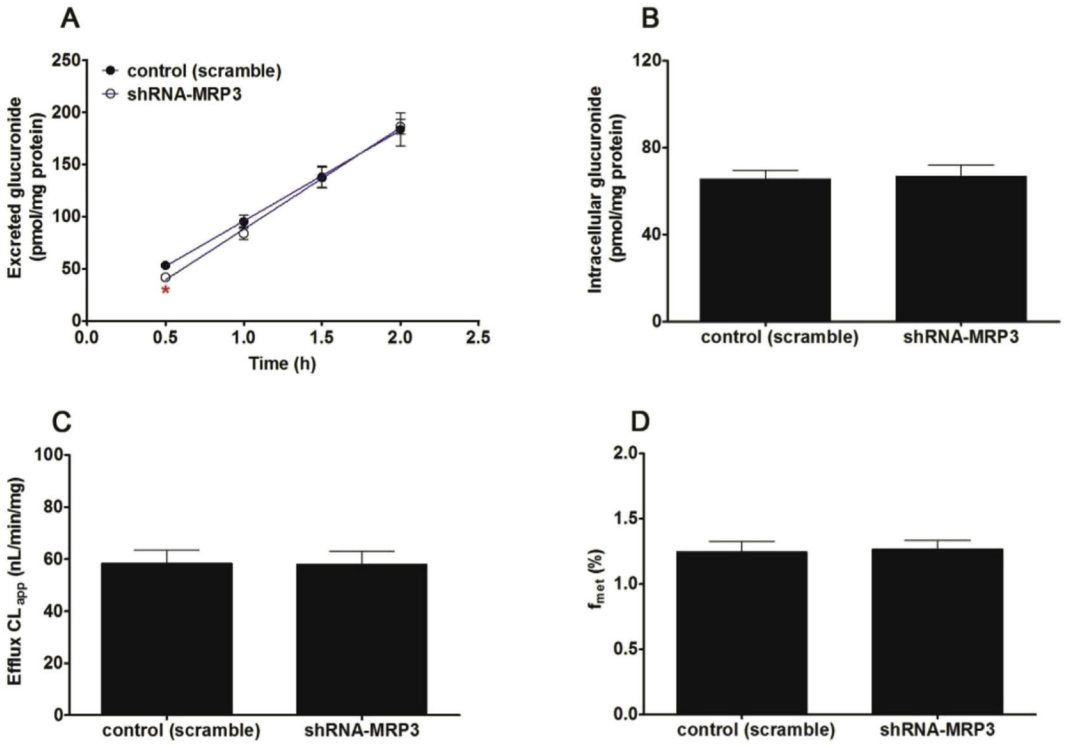

Fig. 12. Effects of shRNA-mediated MRP3 silencing on cycloicaritin-3-*O*-glucuronide excretion and cellular glucuronidation.

(A) Effects of MRP3 silencing on the excretion rates of CICT-3-G; (B) Effects of MRP3 silencing on the intracellular levels of CICT-3-G; (C) Effects of MRP3 silencing on the efflux clearances ($CL_{ef,app}$) of CICT-3-G; (D) Effects of BCRP silencing on cellular glucuronidation (or f_{met}) of CICT-3-G; CICT-3-G, cycloicaritin-3-*O*-glucuronide; All experiments were performed in triplicate (n = 3). (* Parameters of CICT-3-G in engineered HeLa1A1 cells were compared with the same parameters in control group, $*p < 0.05$, $**p < 0.01$, $***p < 0.001$).

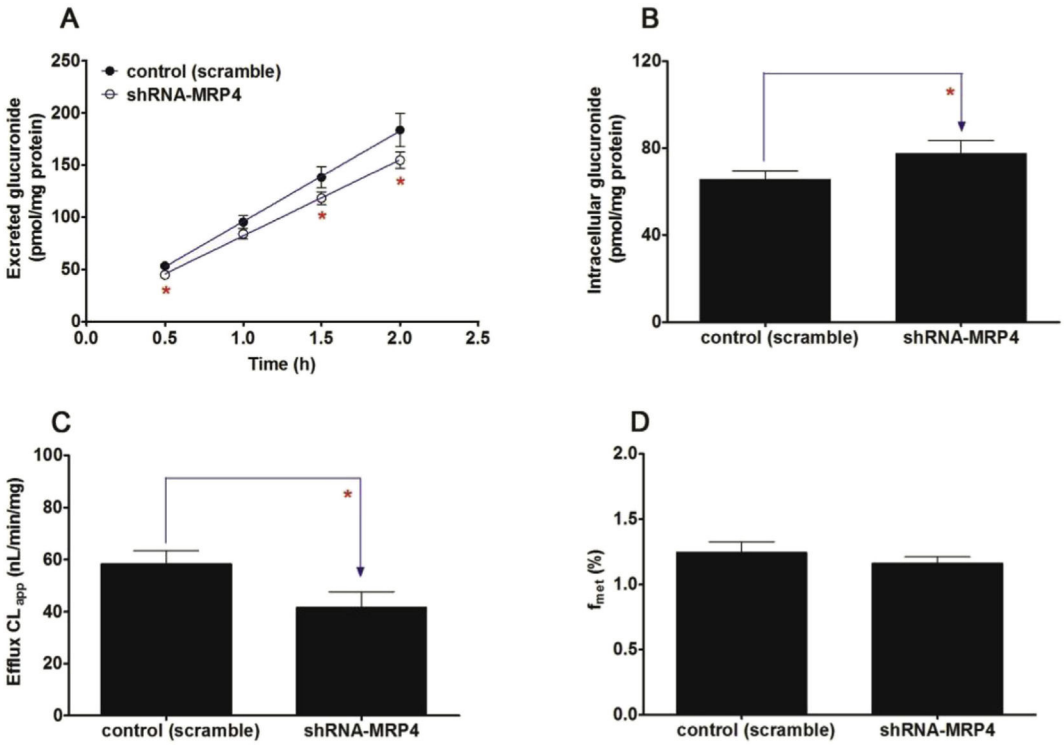

Fig. 13. Effects of shRNA-mediated MRP4 knock-down on the excretion of cycloicaritin-3-*O*-glucuronide and cellular glucuronidation.

(A) Effects of MRP4 knock-down on the excretion rates of CICT-3-G; (B) Effects of MRP4 knock-down on the intracellular levels of CICT-3-G; (C) Effects of MRP4 knock-down on the efflux clearances ($CL_{ef,app}$) of CICT-3-G; (D) Effects of MRP4 knock-down on cellular glucuronidation (or f_{met}) of CICT-3-G. CICT-3-G, cycloicaritin-3-*O*-glucuronide; All experiments were performed in triplicate (n = 3). (* Parameters of CICT-3-G in engineered HeLa1A1 cells were compared with the same parameters in control group, $*p < 0.05$, $**p < 0.01$, $***p < 0.001$).

Table 1

Relative protein expression of transporters (normalized to the levels of GAPDH) in HeLa1A1 and engineered HeLa1A1 cells based on western blotting. All experiments were performed in triplicate (n = 3).

Protein	control	scramble	BCRP-shRNA	MRP1-shRNA	MRP3-shRNA	MRP4-shRNA
BCRP	0.95 ± 0.06	0.96 ± 0.07	0.25 ± 0.04***	0.98 ± 0.07	0.93 ± 0.08	1.05 ± 0.07
MRP1	0.94 ± 0.08	1.15 ± 0.08	1.00 ± 0.09	0.29 ± 0.08***	0.95 ± 0.11	0.96 ± 0.09
MRP3	1.12 ± 0.08	0.94 ± 0.09	1.01 ± 0.06	0.93 ± 0.11	0.37 ± 0.07***	1.02 ± 0.05
MRP4	0.94 ± 0.06	1.02 ± 0.08	0.92 ± 0.05	1.10 ± 0.07	0.95 ± 0.08	0.49 ± 0.08**
UGT1A1	0.77 ± 0.07	0.73 ± 0.06	0.84 ± 0.10	0.79 ± 0.06	0.87 ± 0.12	0.72 ± 0.09
GAPDH	1	1	1	1	1	1

Note:

* protein levels of corresponding efflux transports in engineered HeLa1A1 cells were compared with these in control HeLa1A1 cells.

* $p < 0.05$

** $p < 0.01$,

*** $p < 0.001$.